ISA Transactions 64 (2016) 56–66

Contents lists available at ScienceDirect

ISA Transactions

journal homepage: www.elsevier.com/locate/isatrans

Design of a fractional order PID controller using GBMO algorithm for load–frequency control with governor saturation consideration

Abbasali Zamani, S. Masoud Barakati *, Saeed Yousofi-Darmian

Department of Electrical and Computer Engineering, University of Sistan and Baluchestan, Zahedan, Iran

ARTICLE INFO

Article history:
Received 23 September 2015
Received in revised form
3 April 2016
Accepted 21 April 2016
Available online 9 May 2016
This paper was recommended for publication by Dr. Y. Chen

Keywords:
Load–frequency control
Fractional order PID controller
GBMO algorithm
PID controller
Fuzzy controller

ABSTRACT

Load–frequency control is one of the most important issues in power system operation. In this paper, a Fractional Order PID (FOPID) controller based on Gases Brownian Motion Optimization (GBMO) is used in order to mitigate frequency and exchanged power deviation in two-area power system with considering governor saturation limit. In a FOPID controller derivative and integrator parts have non-integer orders which should be determined by designer. FOPID controller has more flexibility than PID controller. The GBMO algorithm is a recently introduced search method that has suitable accuracy and convergence rate. Thus, this paper uses the advantages of FOPID controller as well as GBMO algorithm to solve load–frequency control. However, computational load will higher than conventional controllers due to more complexity of design procedure. Also, a GBMO based fuzzy controller is designed and analyzed in detail. The performance of the proposed controller in time domain and its robustness are verified according to comparison with other controllers like GBMO based fuzzy controller and PI controller that used for load–frequency control system in confronting with model parameters variations.

1. Introduction

Nowadays, suitable power system reliability and stability against both internal and external disturbances are become more important topics. Constant system frequency or minimum deviation of it, is one of the main quality specifications in power system operation. In a power grid, a significant reduction in frequency will result in high magnetic currents in induction motors and transformers which causes irreparable damages [1].

Frequency stability in a power system depends on balance between generated and consumed active power. As the frequency is common in whole system, any changes in active power demand in some point reflect as frequency change in whole system [1,2]. The control system removes unbalance between generation and consumption by means of automatic changing of generated power, and then keep the frequency and exchanged power constant in rated values, is called Load–Frequency Control (LFC) or Automatic Generation Control (AGC) system.

So far, several methods has been proposed in order to solve LFC problem in power systems. The PID controller is one of the most common controllers used for LFC which some of its classic design methods are discussed in [1–3]. Increasingly growth of intuitive optimization algorithms has attracted the attention of many researchers to use these algorithms in design problems. For instance, in [4,5] Hybrid Particle Swarm Optimization (HPSO) and Bacterial Foraging Optimization (BFO) algorithms are used to design optimal PID controller in a two-area power system.

Recently, using robust control methods in LFC system are taken into consideration [6–9]. In [6], a robust controller is designed for LFC system using Kharitonov's theory. In [7–9], robust control methods are used to design robust PID controller for LFC problem. Using intelligent methods in LFC design for power systems has grown substantially, e.g., artificial neural network [10], fuzzy logic controllers [11] and type-2 fuzzy logic controllers [12]. Also, in [13,14] adaptive controllers are used for LFC problem.

Fractional Order PID (FOPID) is generalized type of conventional PID controller. In this controller, derivative and integrator parts have non-integer orders and so the order should be determined by designer. As a result, the controller would have five parameters to be determined. Some of design methods for FOPID controller are, designing controller based on quantity feedback [15] and root locus [16] theories. In [17–19], optimization algorithms are used to design FOPID controllers. In [17], FOPID controller is designed based on Chaotic Ant Swarm (CAS) algorithm in order to control automatic voltage regulator (AVR) system and its performance is compared with conventional PID controller. FOPID controller design using PSO algorithm for AVR system is done on [18] according to time domain

* Correspondence to: Department of Electrical and Computer Engineering, University of Sistan and Baluchestan, Zahedan, P. O. Box 987-98155, Iran. Tel.: +98 54 31136633.
E-mail addresses: a.zamani@pgs.usb.ac.ir (A. Zamani), smbaraka@ece.usb.ac.ir (S.M. Barakati), saeed.yousofi@pgs.usb.ac.ir (S. Yousofi-Darmian).

http://dx.doi.org/10.1016/j.isatra.2016.04.021
0019-0578/

performance indices. In [19], FOPID controller design is studied with multi-objective optimization algorithms.

In most of abovementioned methods linear model of power system is considered and non-linearity limitations are neglected. In this paper, FOPID controller is designed by Gases Brownian Motion Optimization (GBMO) method which is used to LFC for frequency deviation reduction and improving dynamical performance of two-area power system. GBMO algorithm is a newly introduced and effective method to solve optimization problems. Governor saturation limit (which is a non-linear limitation) is considered in two-area power system model. In addition, design of a fuzzy logic controller based on GBMO algorithm is presented for LFC. Several simulations are done in order to evaluate the performance and robustness of the proposed method. Also, simulation results are compared with some other controllers proposed in the literature.

Rest of the paper is organized as follows. In Section 2, GBMO algorithm is briefly addressed. In Section 3, two-area power system with governor saturation limitation is introduced. The design method of GBMO based FOPID is explained in Section 4. Fuzzy-Logic Controller (FLC) which designed based on GBMO algorithm is also presented in Section 5. Section 6 is dedicated to simulation results and numerical studies. Finally, Section 7 presents some conclusions.

2. Gases Brownian Motion Optimization algorithm (GBMO)

Gases Brownian Motion Optimization algorithm is introduced in [20]. The basis of this algorithm are brownian and vibrating motion of particles in a place. Molecular movement in gases has brownian nature and so, there is no specified direction for molecular velocity but irregularly distributed among all directions. Molecular collision continuously changes both the direction and velocity of them and so the velocity of gas molecules are significantly different. Brownian nature of gas molecules causes them travel whole space rapidly. In [20], it is shown that the GBMO algorithm has a good performance to solving various functions and satisfiability problems. Owing to the efficient search technique of GBMO algorithm in optimization problems with large dimensions, it operates more successful than some other well-known heuristic search algorithms such as: particle swarm optimization (PSO), genetic algorithm (GA), imperialist competitive algorithm (ICA), and gravitational search algorithm (GSA). Run time of the GBMO algorithm is shorter than GA, GSA, and ICA but it is slightly longer than PSO. The GBMO algorithm has linear time complexity. Also, it is shown that, with increase of molecules number the quality of solutions is improved while the run time is increased.

The stages of this algorithm are as follows [20]:

i. Some gas molecules are randomly generated in search space.
ii. For each molecule some random radiuses are generated in [0 1] interval.
iii. The system temperature which is the parameter for indexing the algorithm convergence, is initialized. Temperature in the beginning of the algorithm is high and decreases gradually. In the beginning of the algorithm, according to high kinetic energy velocity molecules travel in wider interval. Over time and decreasing in temperature, kinetic energy and velocity of molecules movement, the search will done in shorter interval.
iv. The velocity and location of molecules are calculated and updated according to following:

$$v_i^d(t+1) = v_i^d(t) + \sqrt{\frac{3kT}{m}},$$
$$x_i^d(t+1) = x_i^d(t) + v_i^d(t+1), \quad (1)$$

where $v_i^d(t), x_i^d(t)$ are dth dimension velocity and location of ith molecule in tth epoch, respectively.

v. The competency of each location is calculated by cost function.
vi. Each molecule addition to move in different directions, has a vibrating motion in a specified radius. Each molecule's swing is local in beginning of the algorithm and become more global in final steps. These swings are obtained as follows,

$$x_i^d(t+1) = x_i^d(t) + b - \left(\frac{a}{2\pi}\right)\sin(2\pi\theta_n)\mathrm{mod}(1), \quad (2)$$

where $a=0.5$ and $b=0.2$.
vii. Again, the competency of each location is calculated by cost function.
viii. Updating the mass and temperature according to (3).

$$worst(t) = \min_{i\in\{1,2,\ldots,N\}} fit_i(t),$$
$$best(t) = \max_{i\in\{1,2,\ldots,N\}} fit_i(t),$$
$$m_i(t) = \frac{fit_i(t) - worst(t)}{best(t) - worst(t)}, \quad (3)$$
$$T = T - \left(\frac{1}{mean(fit_i(t))}\right).$$

In (3), $fit_i(t)$ is the competency of molecule i in tth epoch.
ix. The algorithm is repeated until the stopping criterion is satisfied.

Two stop criteria could be imagined for this algorithm. One can be decreasing the temperature (T) and yielding to a small enough value like ε and other one can be receiving a specific epoch. At initial

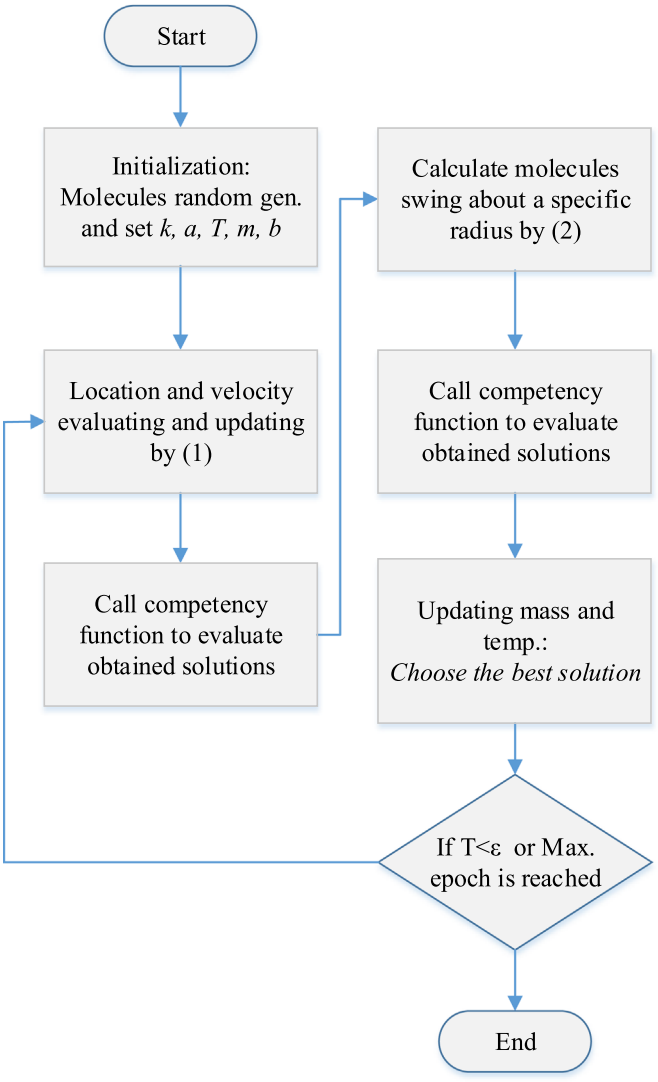

Fig. 1. GBMO algorithm flowchart.

epochs, the system temperature and so the kinetic energy and velocity of molecules are high. As a result, gases Brownian motion causes global exploration of whole search space and turbulent rotational motion will have a good performance to local exploration. By lapse of time and decreasing the system temperature, gases Brownian motion will decrease. In low temperatures, the turbulent rotational motion mainly causes global search and the gases Brownian motion has a significant role in the local search of the problem space. This role exchange (because of temperature decrease) allows a good compromise between exploration and exploitation. Flowchart of the algorithm is illustrated in Fig. 1.

3. Two-area power system model

Some non-linear elements in power system such as dead bands, limitation in generating rate constraint, and governor limits have significant impact on stability. In order to increase security and because of practical limitations in power system, in the governor modeling some limits should be considered. A two-area Load–Frequency Control (LFC) system along with governor limits is illustrated in Fig. 2. In this system, $M_i=2H_i$ where H_i is inertia constant, D_i is load-damping constant, R_i is regulation constant, τ_{Ti} is turbines' time-constant, and τ_{gi} is governors' time-constant for ith system.

In normal operation state, power system is operated so that the demand of both areas supplied in nominal frequency. A normal two-area LFC system is work according to control the tendency of tie-line, i.e., tending of each area to decrease Area Control Error (ACE) to zero. The ACE for each area is a linear combination of frequency error and power change as:

$$\begin{aligned} ACE_1 &= \Delta P_{12} + B_1 \Delta f_1, \\ ACE_2 &= \Delta P_{21} + B_2 \Delta f_2, \end{aligned} \tag{4}$$

where $B_i = \frac{1}{R_i} + D_i$, ΔP_{12} and ΔP_{21} are differences between planned power exchange with actual power exchange from area 1 to area 2 and vice versa ($\Delta P_{12} = -\Delta P_{21} = \Delta P_{tie}$). ACEs are used as actuator signals to enable change in set points of power reference. Δf_i is the frequency deviation of ith area and in steady state ΔP_{tie} and Δf_i will be zero.

4. FOPID controller design procedure

FOPID controller is introduced by Podlubny in [21]. This kind of controllers attracts significant attention owing to better performance than conventional PID controllers. In fact, presence of five parameters to choice increases design flexibility and allows designer to more suitable shaping of open-loop transfer function for a special control task. In the literature, it is shown that the FOPID controllers have better responses than PID ones in both integer and fractional order systems [22]. However, tuning the FOPID controllers in term of design and stability analysis is more complex. To deal with this issue, different designing approaches are introduced in the literature [16,23–25]. This controller has a transfer function like (5).

$$G_c(s) = K_P + \frac{K_I}{s^{\lambda}} + K_D s^{\mu}. \tag{5}$$

In (5), if $\lambda=1$ and $\mu=1$ the standard PID controller will be obtained. Also, if $\lambda=1$ and $\mu=0$ the standard PI, if $\lambda=0$ and $\mu=1$ the standard PD and if $\lambda=0$, and $\mu=0$ the standard proportional (P) controller will be obtained. So, all types of PID controller are special cases of FOPID controller.

Design parameters in FOPID controller are K_P, K_I, K_D, λ and μ. As a result, in order to design the FOPID controller location of each

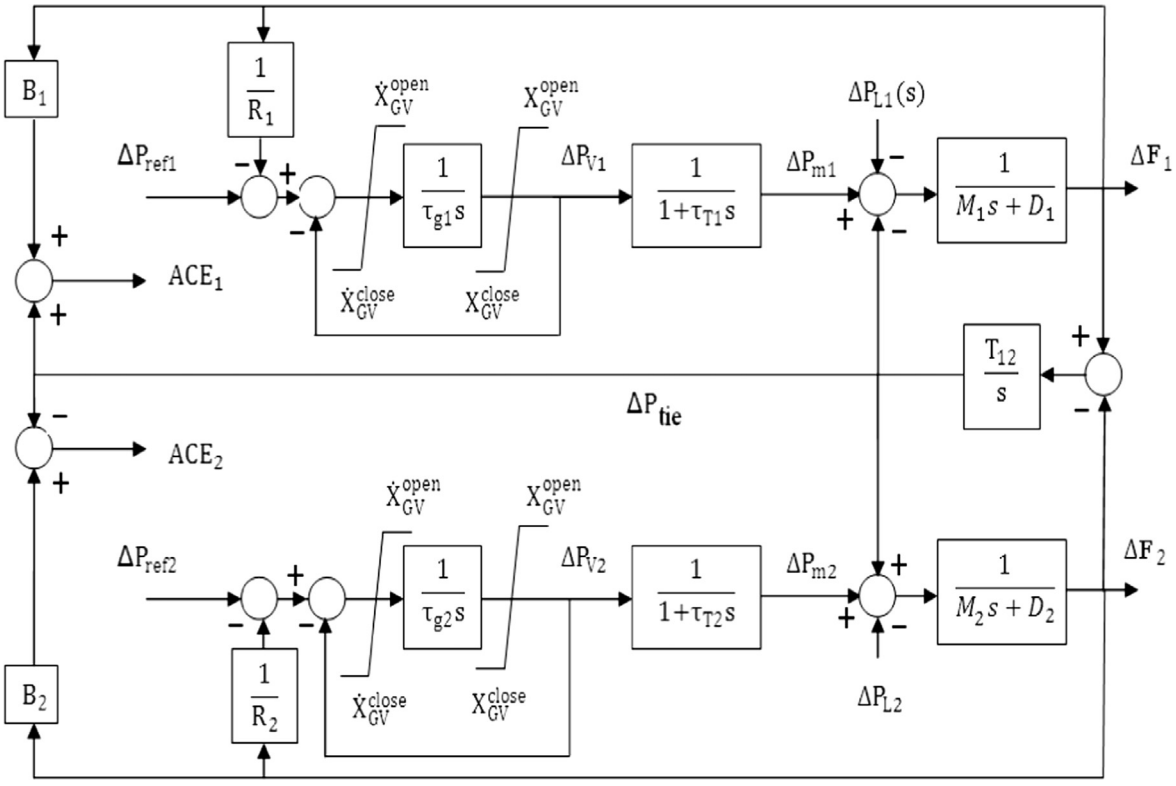

Fig. 2. Two-area power system with governor saturation limit.

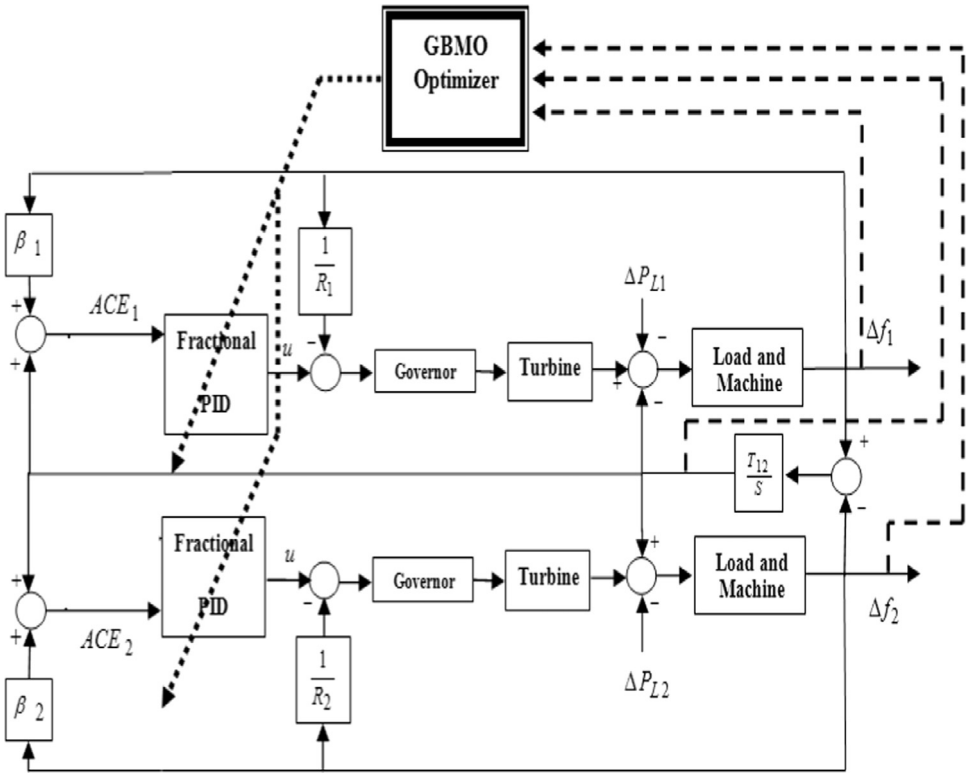

Fig. 3. Design block diagram of GBMO-FOPID.

molecule is considered as,

$$x_i(t) = \left[K_{P1}K_{I1}K_{D1}\lambda_1\mu_1 K_{P2}K_{I2}K_{D2}\lambda_2\mu_2\right]^T. \quad (6)$$

Various cost functions are exists in order to optimal design of controller for LFC system [26,27]. In (7), three widely used cost functions are shown which lead to improve system performance in steady state and improve transient response of closed loop system. J_1 is Integral of Squared Error (ISE), J_2 is Integral of Absolute Error (IAE) and J_3 is Integral of Time multiply by Absolute Error (ITAE). In literature, it's reported that J_3 is better than others mainly because of the ability to mitigate overshoot and settling time [9]. So, performance index J_3 is used which is integral of time multiply absolute error (ITAE) of the frequency deviation of both areas and tie-line power. In (7), ΔP_{tie} is deviation in tie-line power, Δf_i, $i=1$, 2 is deviation in the ith system frequency and T_{sim} is the simulation time.

$$\begin{aligned} J_1 &= ISE = \int_{t=0}^{t=T_{sim}} \left(|\Delta P_{tie}| + |\Delta f_1| + |\Delta f_2|\right)^2 dt, \\ J_2 &= IAE = \int_{t=0}^{t=T_{sim}} \left(|\Delta P_{tie}| + |\Delta f_1| + |\Delta f_2|\right) dt, \\ J_3 &= ITAE = \int_{t=0}^{t=T_{sim}} t \cdot \left(|\Delta P_{tie}| + |\Delta f_1| + |\Delta f_2|\right) dt. \end{aligned} \quad (7)$$

Then, the optimization problem is in form of (8) which higher limit of K_P, K_I and K_D is 20 and for λ and μ is 2. In order to solve this problem GBMO algorithm is used. As shown in Fig. 3, GBMO optimizer tune the FOPID controller to achieve proper performance.

$$\begin{aligned} &Min \quad J_3 \\ &Subject \quad to \quad 0 \le K_{Pi} \le 20 \\ &\qquad\qquad 0 \le K_{Ii} \le 20 \\ &\qquad\qquad 0 \le K_{Di} \le 20 \\ &\qquad\qquad 0 \le \lambda_i \le 2 \\ &\qquad\qquad 0 \le \mu_i \le 2 \\ &\qquad\qquad i = 1, 2 \end{aligned} \quad (8)$$

The design procedure of the FOPID controller based on the GBMO algorithm is as follows:

Step 1: determine the parameters of LFC system.
Step 2: set the parameters of GBMO algorithm.
Step 3: specify the lower and upper bounds of the 10 controller parameters for Two-Area.
Step 4: randomly generate gas molecules within the range of each controller parameter and random radiuses in [0 1] interval.
Step 5: for each molecule, calculate the integer-order approximation transfer function of FOPID controller using Oustaloup's method and apply the integer-order approximation transfer function of FOPID controller to the LFC system.
Step 6: evaluate the fitness of each molecule using J_3 in Eq. (7).
Step 7: the velocity and location of molecules are calculated and updated according to Eq. (1).
Step 8: for each molecule, calculate the integer-order approximation transfer function of FOPID controller using Oustaloup's method and apply the integer-order approximation transfer function of FOPID controller to the LFC system.
Step 9: evaluate the fitness of each molecule using J_3 in Eq. (7).
Step 10: calculate the molecule's swing using Eq. (2) for local search.
Step 11: for each molecule, calculate the integer-order approximation transfer function of FOPID controller using Oustaloup's method and apply the integer-order approximation transfer function of FOPID controller to the LFC system.
Step 12: evaluate the fitness of each molecule using J_3 in Eq. (7).
Step 13: updating the mass and temperature according to Eq. (3).
Step 14: go to Step 7 until the temperature is reached to ε or maximum epoch is reached.

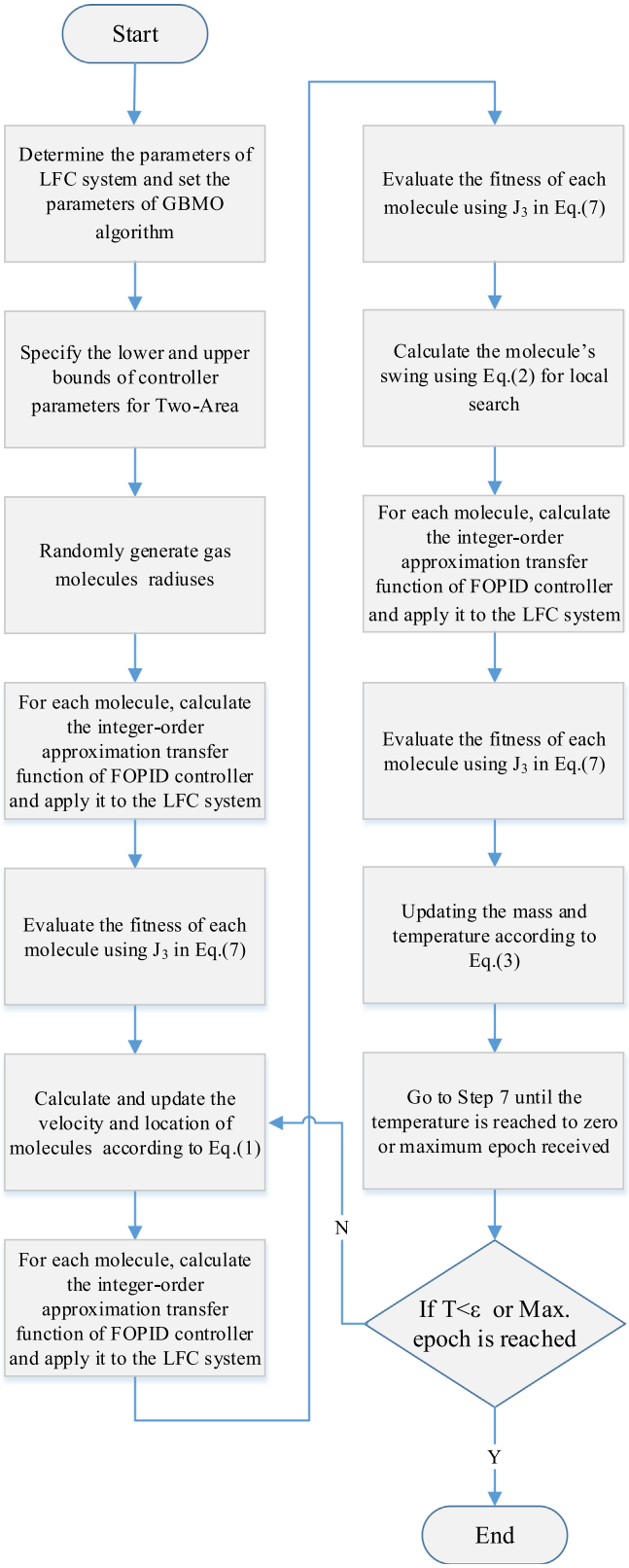

Fig. 4. Flowchart of GBMO-FOPID design procedure.

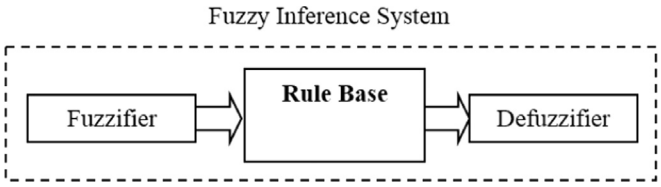

Fig. 5. Main structure of fuzzy controller.

Oustaloup's method is briefly explained in Appendix A. In order to better understanding, the design procedure of the proposed strategy is depicted in Fig. 4.

5. Fuzzy logic controller

In order to compare the performance of the GBMO-FOPID, fuzzy logic controller (FLC) tuned by GBMO algorithm for LFC will introduced in this section. Main structure of a FLC is shown in Fig. 5. Because of non-linear and complex nature and multi-variable conditions of modern power systems, conventional control approaches may have not satisfactory results. Because of robustness and more reliability of FLCs, they are useful for wide range of control problems in power systems [28–30]. In this paper, an auto-tuned FLC based on GBMO algorithm is proposed in order to solve the LFC problem. In the following, structure of fuzzy logic load–frequency controller and its' optimization method based on GBMO algorithm are introduced.

5.1. Fuzzy LFC structure

Main structure of a FLC is consists of four components as, fuzzifier, inference system, knowledge base, and defuzzifier. In the beginning, fuzzifier transforms input signals to fuzzy values. These values are input of inference system, which uses a fuzzy reasoning mechanism in order to calculate fuzzy value of output signals. This fuzzy value is obtained from making appropriate decisions. Knowledge base contains fuzzy rule sets and Membership Functions (MFs) which known as "Rule Table". Finally, modified output sets are transformed to non-fuzzy signal by means of defuzzifier. Adoption of a suitable set of MFs and fuzzy rules by means of human experience is computationally time-consuming and costly. Also, suitable design of fuzzy rules and proper setting of FLCs' parameters are key factors to obtain satisfactory control performance.

5.2. Fuzzy LFC optimization method

In this paper, an auto-tuning based GBMO algorithm for optimal and simultaneously setting of MFs and fuzzy control rules is developed. For this purpose, the design problem is restructured as an optimization problem and the GBMO algorithm is used to solve it. In order to combine GBMO algorithm with fuzzy LFC design, MFs and fuzzy rule sets should be coded in form of a solution array and cost function should be defined such that the design criteria achieve through minimizing it. The fuzzy load frequency controller scheme is depicted in Fig. 6. It can be seen that, fuzzy controllers actually are proportional-derivative based fuzzy (FPD) controllers. It is worth mentioning, differences between the FOPID and FPD controllers can be described as follows:

- in spite of FOPID controller, derivative part of the FPD has an integer order.
- the FOPID controller coefficients are directly tuned by GBMO algorithm, while in FPD, signals of proportional and derivative sections (ACE_i and $d(ACE_i)/dt$, respectively) are used as inputs of

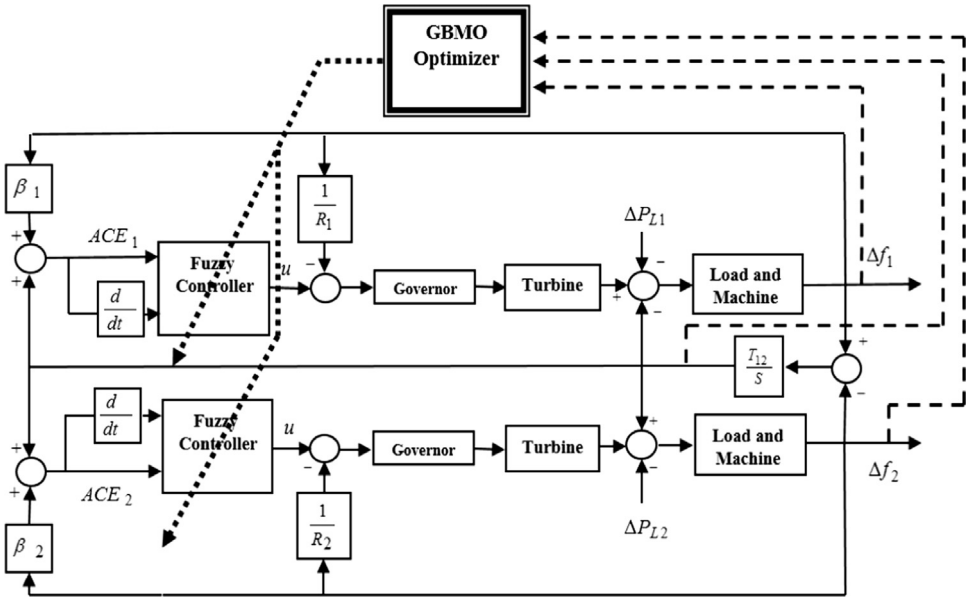

Fig. 6. FPD controller used for LFC in two-area power system.

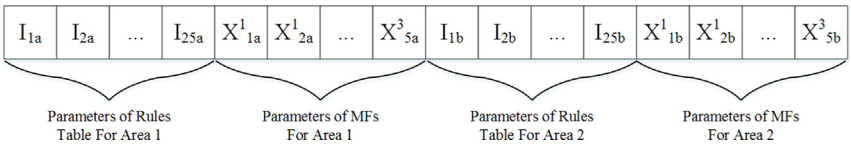

Fig. 7. Basic code structure for GBMO algorithm.

Table 1
The rule base of fuzzy controller in code structure.

Input 2	Input 1				
	NM	NS	Z	PS	PM
NM	I_1	I_2	I_3	I_4	I_5
NS	I_6	I_7	I_8	I_9	I_{10}
Z	I_{11}	I_{12}	I_{13}	I_{14}	I_{15}
PS	I_{16}	I_{17}	I_{18}	I_{19}	I_{20}
PM	I_{21}	I_{22}	I_{23}	I_{24}	I_{25}

fuzzy controller and the parameters of fuzzy controller are tuned by GBMO algorithm.

Parameters which should be simultaneously optimized by GBMO algorithm, are: normalizing factors, centers and widths of triangular MFs, as well as fuzzy rules. The code structure for GBMO algorithm is illustrated in Fig. 7. In this figure, parameters of fuzzy rules and MFs are: I_j, $j=1, 2,\ldots,25$ and X_z^k, $k=1, 2, 3$, $z=1,\ldots, 5$, respectively.

Assume that FLC output has five MFs as, {*NM, NS, ZE, PS, PM*} which express with {0, 1, 2, 3, 4} indices. As a result, rules of fuzzy controllers can be obtained as illustrated in Table 1. For instance, $I_3=3$ means the control rule presents as follows:

*IF Input*1 *is ZE and Input*2 *is NM THEN Output is PS.*

Membership functions of FLC consist of two trapezoidal and three triangular MFs with five parameters $X_{1,\ldots}X_5$ that are shown in Fig. 8. For instance, X_2^1 is the second parameter of first input of the FLC.

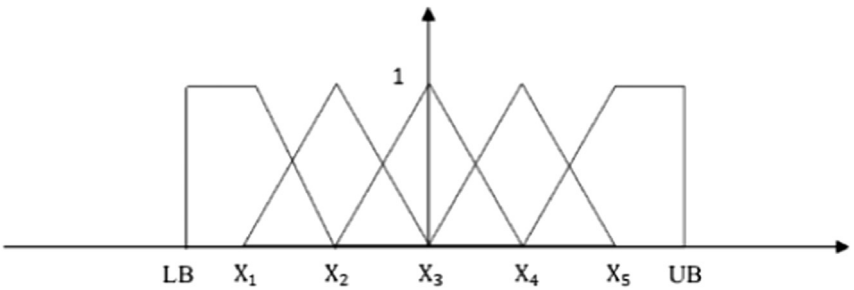

Fig. 8. Considered membership function in code structure.

Table 2
The optimal rule base of fuzzy controller obtained by GBMO for area 1.

ACE_1	$dACE_1/dt$				
	NM	NS	Z	PS	PM
NM	*PM*	*PM*	*NS*	*PS*	*Z*
NS	*PM*	*NS*	*PS*	*NM*	*PS*
Z	*Z*	*PS*	*PS*	*PM*	*Z*
PS	*NS*	*NM*	*PS*	*NM*	*PS*
PM	*NS*	*Z*	*PM*	*Z*	*PM*

Table 3
The optimal rule base of fuzzy controller obtained by GBMO for area 2.

ACE_2	$dACE_2/dt$				
	NM	NS	Z	PS	PM
NM	*PM*	*PM*	*PM*	*PM*	*NM*
NS	*PM*	*PM*	*Z*	*NS*	*PS*
Z	*NS*	*PS*	*NM*	*PM*	*PM*
PS	*Z*	*Z*	*NS*	*Z*	*PS*
PM	*PS*	*Z*	*PS*	*NS*	*NM*

Table 4
The optimal parameters of fuzzy variables obtained by GBMO algorithm.

MFs' parameters for Area 1														
X^1_{1a}	X^1_{2a}	X^1_{3a}	X^1_{4a}	X^1_{5a}	X^2_{1a}	X^2_{2a}	X^2_{3a}	X^2_{4a}	X^2_{5a}	X^3_{1a}	X^3_{2a}	X^3_{3a}	X^3_{4a}	X^3_{5a}
−0.891	−0.238	−0.2	0.479	0.781	−0.7	−0.2	0.201	0.391	0.617	−0.856	−0.228	−0.034	0.5	0.843
MFs' parameters for Area 2														
X^1_{1b}	X^1_{2b}	X^1_{3b}	X^1_{4b}	X^1_{5b}	X^2_{1b}	X^2_{2b}	X^2_{3b}	X^2_{4b}	X^2_{5b}	X^3_{1b}	X^3_{2b}	X^3_{3b}	X^3_{4b}	X^3_{5b}
−0.886	−0.203	0.162	0.459	0.812	−0.71	−0.203	0.199	0.231	0.913	−0.5	−0.415	−0.197	0.356	0.885

Table 5
Simulated FOPID controller coefficients.

Controller	Area	K_p	K_i	K_d	μ	λ
GBMO-FOPID	1	11.23	16.62	7.0	0.99	0.99
	2	0.05	3.64	5.82	0.65	1.31
FOPID Prop. In [31]	1	4.67	19.23	4.62	0.7	1.3
	2	2	0	12.25	0.8	1.5

Lower and upper values of MFs and fuzzy rules in solution vector are considered as following:

$$0 < K_i \le 1, \quad i = 1,2$$
$$0 \le I_j < 5, \quad j = 1,\ldots,25$$
$$-1 < X_z^k < 1, \quad k = 1,2,3 \quad z = 1,\ldots,5.$$

The optimal knowledge base obtained from GBMO algorithm for area 1 and area 2 are depicted in Tables 2 and 3, respectively. MFs of ACE_i, $d(ACE_i)/dt$, $i=1, 2$ and output variable for area 1 and area 2 are illustrated in Table 4.

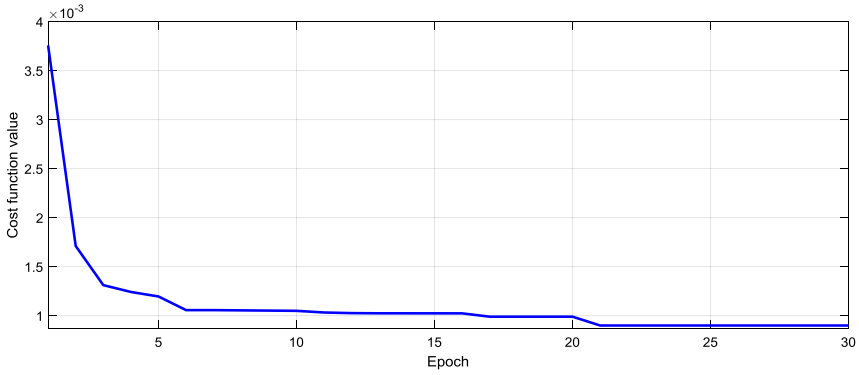

Fig. 9. Convergence of the algorithm.

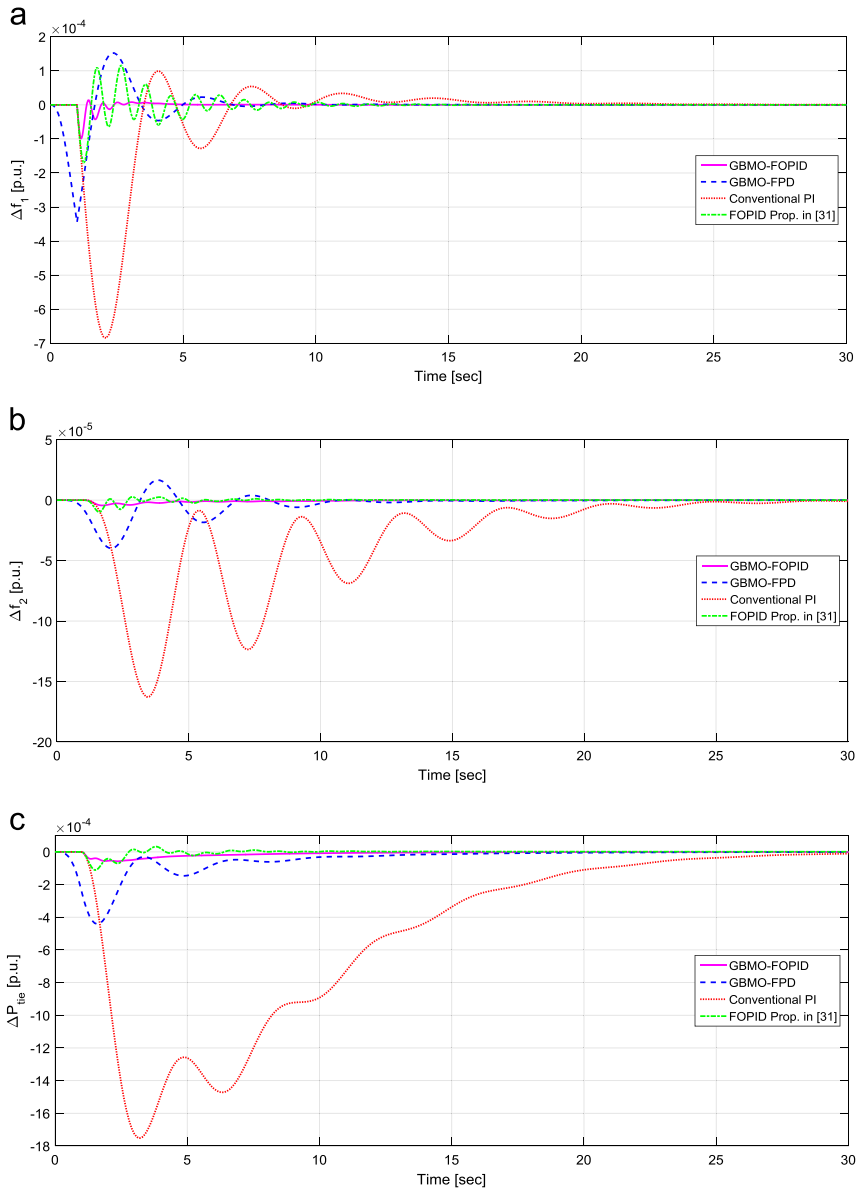

Fig. 10. Simulation results when nominal parameters used: (a) frequency variation in area 1, (b) frequency variation in area 2, and (c) transmitted power variation.

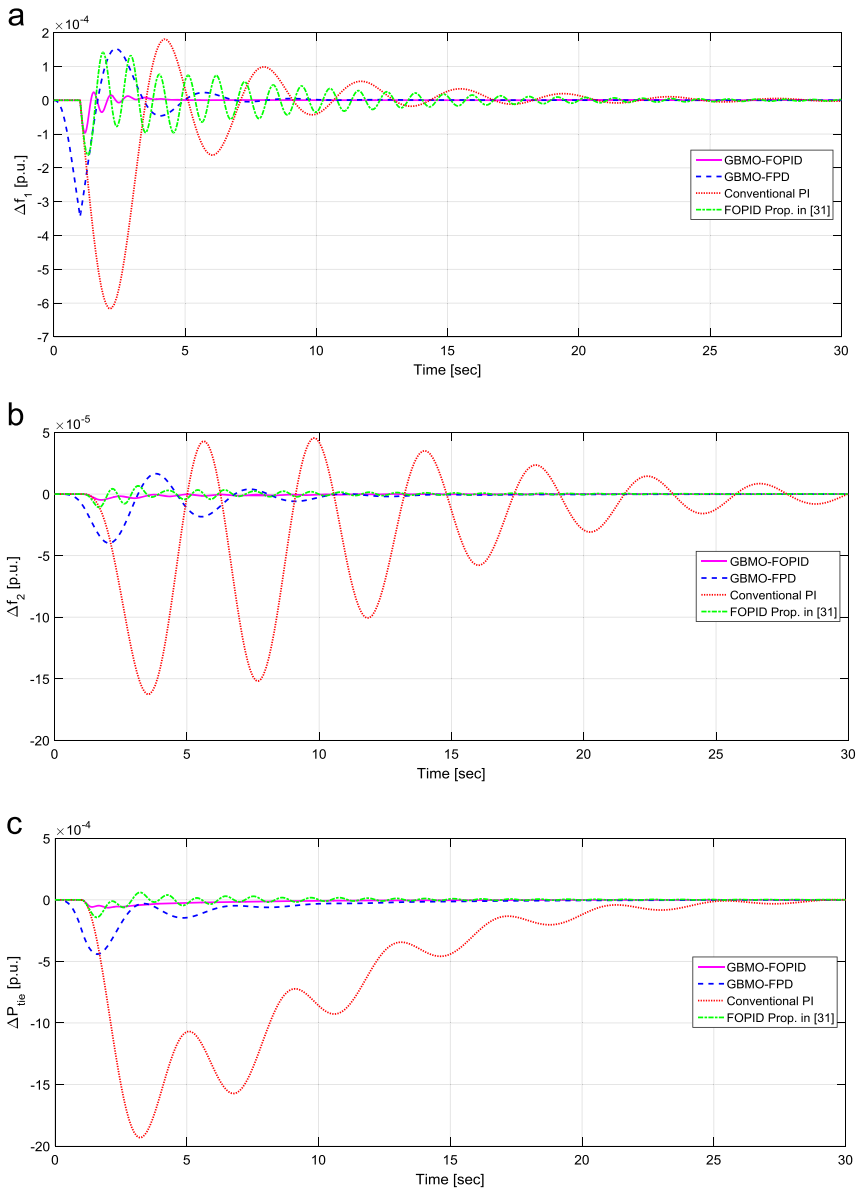

Fig. 11. Simulation results when 20% increase in parameters is occurred: (a) frequency variation in area 1, (b) frequency variation in area 2, and (c) transmitted power variation.

6. Simulation results

In order to simulate the system with GBMO algorithm, 100 gas molecules with initial temperature of 30 °C, $a=0.5$ and $b=0.2$ is considered. The ε is considered to be 0.001 and in simulations it is observed that this criteria achieved before the epoch 30. So the stop criteria in simulations is considered to be the number of epochs (30). For two-area power system, parameters of area 1 are: $M_1=10$, $D_1=0.6$, $\tau_{g1}=0.2$, $\tau_{T1}=0.5$ and $R_1=0.05$ and parameters of area 2 are: $M_2=8$, $D_2=0.9$, $\tau_{g2}=0.3$, $\tau_{T2}=0.6$ and $R_2=0.0625$. Also, limitations considered for governor are: $\dot{X}_{GV}^{close}=1.5$, $\dot{X}_{GV}^{open}=0.4$, $X_{GV}^{close}=0.4$ and $X_{GV}^{open}=1.2$. It is worth mentioning that in simulations, disturbance is considered as a step of 0.01 p.u amplitude. Results of simulation for obtaining FOPID coefficients after 30 epochs is shown in Table 5 and convergence of the algorithm is shown in Fig. 9.

In order to better approximate of FOPID controller with an integer-ordered transfer function, frequency interval of $[f_l=0.01\ f_h=100]$ and number of corner frequencies $N=5$ are selected. For evaluate the performance of designed controllers, the FPD controller based on GBMO algorithm, which described in previous section, PI controller according to [1] with $K_{i1}=K_{i2}=0.3$, and FOPID tuned based on method proposed in [31] with coefficients bring in Table 5 also considered and applied to two-area power system of Fig. 2, and the system is simulated for 30 s. Fig. 10 shows simulation results when nominal parameters of system are used. As it can be seen, GBMO-FOPID controller has superior performance than all other controllers and the conventional PI controller has the worst responses.

In order to evaluate the robustness of proposed method against system parameter variations from nominal values, effect of two type of variation in parameters is considered. In first case, performance of the proposed method is investigated for

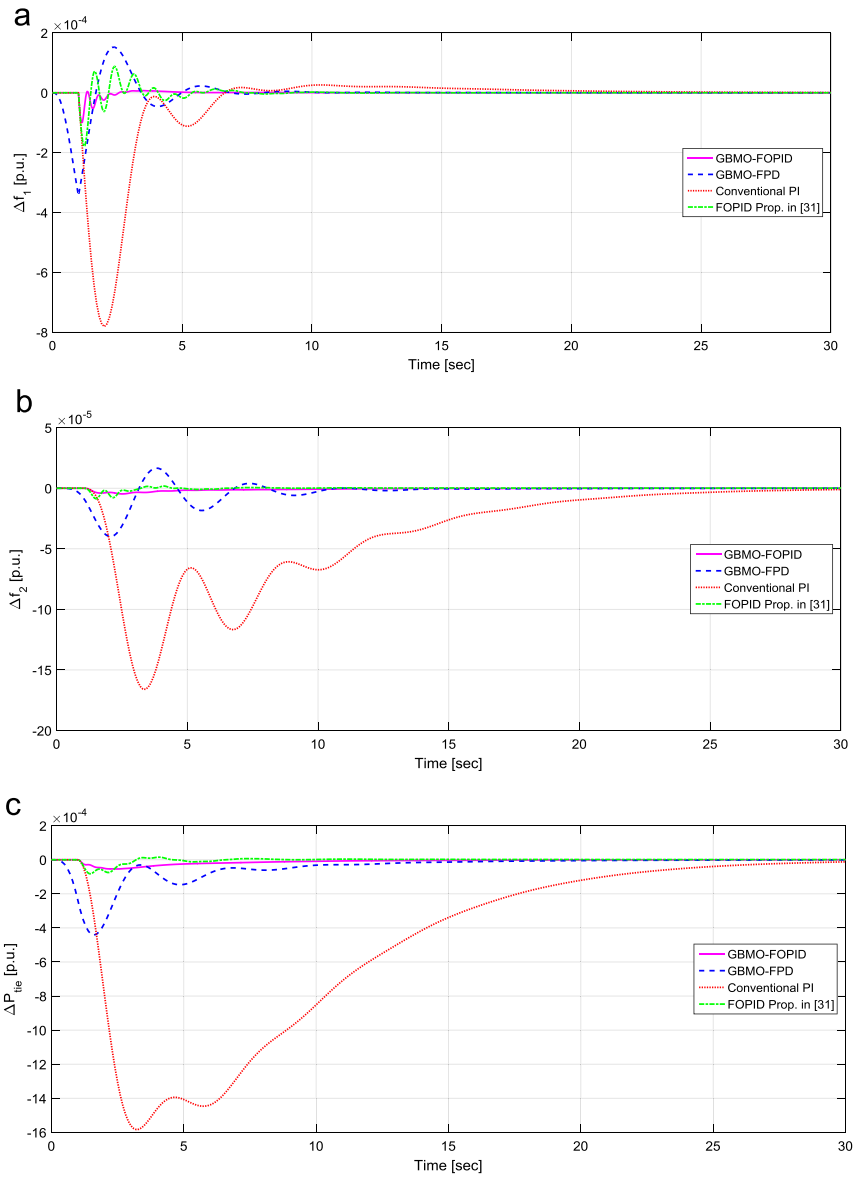

Fig. 12. Simulation results when 20% decrease in parameters is occurred: (a) frequency variation in area 1, (b) frequency variation in area 2, and (c) transmitted power variation.

increase of 20% in model parameters. Response of the system to these increases in parameters from nominal values are illustrated in Fig. 11. It can be observed that the conventional PIs' response is worse than the nominal (without parameter variations) case. In second case, performance of the proposed method is investigated for decreasing 20% in model parameters. Response of the system to decreasing of parameters from nominal values are illustrated in Fig. 12. Again here, the response of conventional PI is worse than nominal case. Simulation results show that despite of 20% change in parameters, FOPID controllers have superior performance than both FPD and classic PI controllers. Also, it is concluded that FPD controller has very better responses than PI controller. For better comparison, numerical results of all simulations are depicted in Table 6. As shown in the Table 6, the GBMO algorithm helps the FOPID controller to be more robust than FOPID. Also, one can observe that, the GBMO-FOPID have the best robustness and performance over other controllers and generally FOPID controller has better performance than FPD and conventional PI controllers.

7. Conclusion

In this paper, a fractional order PID controller based on Gases Brownian Motion Optimization algorithm for load–frequency control problem is proposed. In addition, a fuzzy PD controller based on GBMO algorithm is presented in detail. In LFC system the governor saturation is considered. Simulation results prove that proposed GBMO-FOPID and GBMO-FPD controllers have superior performance than classic PI controller and generally FOPID controllers are the best. Also, it is shown that in spite of 20% change in system parameters response of the system with GBMO-FOPID and GBMO-FPD controllers still good and proven that system is robust against parameters changes with these proposed controllers.

Table 6
Simulation results of all controllers under different conditions.

Test condition		Under shoot (US), Settling time (ST)	GBMO-FOPID	GBMO-FPD	FOPID [31]	PI
Normal	Δf_1	US($\times 10^{-4}$)	**−0.99**	−3.45	−1.7	−6.85
		ST(sec)	**1.82**	6.25	7.8	15.14
	Δf_2	US($\times 10^{-5}$)	**−0.44**	−3.98	−0.98	−16.3
		ST(sec)	**4.1**	10.1	5.3	27.4
	ΔP	US($\times 10^{-4}$)	**−0.57**	−4.42	−1.12	−17.5
		ST(sec)	5.95	12.9	**5.33**	27.2
20% decrease	Δf_1	US($\times 10^{-4}$)	**−0.99**	−3.45	−1.79	−7.81
		ST(sec)	**1.64**	4.45	3.31	6.23
	Δf_2	US($\times 10^{-5}$)	**−0.47**	−3.98	−0.87	−16.5
		ST(sec)	2.95	9.83	**2.36**	24.8
	ΔP	US($\times 10^{-4}$)	**−0.54**	−4.4	−0.83	−15.8
		ST(sec)	3.91	12.1	**2.52**	26.94
20% increase	Δf_1	US($\times 10^{-4}$)	**−0.97**	−3.45	−1.63	−6.16
		ST(sec)	**1.95**	6.05	13.3	16.13
	Δf_2	US($\times 10^{-5}$)	**−0.48**	−3.98	−1.1	−16.3
		ST(sec)	**3.36**	10.16	9.22	>30
	ΔP	US($\times 10^{-4}$)	**−0.64**	−4.42	−1.43	−19.3
		ST(sec)	**5.92**	12.9	7.69	28.2

Bolded numbers indicate best values over all controllers.

Appendix A

In order to implementation and simulation of fractional order (FO) transfer functions, numerical approximations are the most attractive choices. In these methods the behavior of FO Laplace operator is approximated with integer order transfer functions. An efficient way to approximation of FO transfer functions is Oustaloup's method [32]. In this method, a recurrent distribution of N poles and N zeros is used for approximation purpose in the form of,

$$s^{\alpha} \approx \prod_{n=1}^{N} \frac{1+\frac{s}{\omega_{z,n}}}{1+\frac{s}{\omega_{p,n}}}, \alpha > 0. \quad \text{(A1)}$$

In (A1), $\omega_{z,i}$ and $\omega_{p,i}$ ($i=1,\ldots,N$) are angular frequency of ith zero and pole, respectively. In order to have an authentic approximation, zeros and poles should be located in the frequency range of $[\omega_l, \omega_h]$. In this paper, the Oustaloup's method is used for implementation of FOPID controller in simulation section.

References

[1] Saadat H. Power system analysis. New York: McGraw-Hill; 1999.
[2] Kundur P. Power system stability and control. California: McGraw-Hill; 1994.
[3] Nanda J, Mangla A, Suri S. Some findings on automatic generation control of an interconnected hydrothermal system with conventional controllers. IEEE Trans Energy Convers 2006;21(1):187–93.
[4] Taher S, Hematti R, Abdolalipour A, Tabei SH. Optimal decentralized load frequency control using HPSO algorithms in deregulated power systems. Am J Appl Sci 2008;5(9):1167–74.
[5] Ali ES, Abd-Elazim SM. BFOA based design of PID controller for two area load frequency control with nonlinearities. Electr Power Energy Syst 2013;51:224–31.
[6] Toulabi MR, Shiroei M, Ranjbar AM. Robust analysis and design of power system load frequency control using the Kharitonov's theorem. Electr Power Energy Syst 2014;55:51–8.
[7] Yazdizadeh A, Ramezani MH, Hamedrahmat E. Decentralized load frequency control using a new robust optimal MISO PID controller. Int J Electr Power Energy Syst 2012;35(1):57–65.
[8] khodabakhshian A, Edrisi M. A new robust PID load frequency controller. Control Eng Pract 2008;16(9):1069–80.
[9] Shabani H, Vahidi B, Ebrahimpour M. A robust PID controller based on imperialist competitive algorithm for load–frequency control of power systems. ISA Trans 2013;52(1):88–95.
[10] Saikia LC, Mishra S, Sinha N, Nanda J. Automatic generation control of a multi area hydrothermal system using reinforced learning neural network controller. Int J Electr Power Energy Syst 2011;33(4):1101–10.
[11] Sahu RK, Panda S, Yegireddy NK. A novel hybrid DEPS optimized fuzzy PI/PID controller for load frequency control of multi-area interconnected power systems. J Process Control 2014;24(10):1596–608.
[12] Sabahi K, Ghaemi S, Pezeshki S. Application of type-2 fuzzy logic system for load frequency control using feedback error learning approaches. Appl Soft Comput 2014;21:1–11.
[13] Zribi M, Al-Rashed M, Alrifai M. Adaptive decentralized load frequency control of multi-area power systems. Int J Electr Power Energy Syst 2005;27(8):575–83.
[14] Ford JJ, Bevrani H, Ledwich G. Adaptive load shedding and regional protection. Int J Electr Power Energy Syst 2009;31(10):611–8.
[15] Cervera J, Banos A, Monje C, Vinagre B. Tuning of fractional PID controllers by using QFT. In: Proceedings of the 32nd annual conference on IEEE industrial electronics, 2006. p. 5402–5407.
[16] Biswas A, Das S, Abraham A, Dasgupta S. Design of fractional-order $PI^{\lambda}D^{\mu}$ controllers with an improved differential evolution. Eng Appl Artif Intell 2009;22:343–50.
[17] Tang Y, Cui M, Hua C, Li L, Yang Y. Optimum design of fractional order $PI\lambda D\mu$ controller for AVR system using chaotic ant swarm. Expert Syst Appl 2012;39(8):6887–96.
[18] Panda S, Sahu BK. Design and performance analysis of PID controller for an automatic voltage regulator system using simplified particle swarm optimization. J Frankl Inst 2012;349(8):2609–25.
[19] Pan I, Das S. Chaotic multi-objective optimization based design of fractional order $PI^{\lambda}D^{\mu}$ controller in AVR system. Int J Electr Power Energy Syst 2012;43(1):393–407.
[20] Abdechiri M, Meybodib MR, Bahrami H. Gases Brownian motion optimization: an algorithm for optimization (GBMO). Appl Soft Comput 2013;13(5):2932–46.
[21] Podlubny I. Fractional-order systems and $PI^{\lambda}D^{\mu}$ controllers. IEEE Trans Autom Control 1999;44(1):208–14.
[22] Hamamci SE. An algorithm for stabilization of fractional-order time delay systems using fractional-order PID controllers. IEEE Trans Autom Control 2007;52(10):1964–9.
[23] Zamani M, Karimi-Ghartemani M, Sadati N, Parniani M. Design of fractional order PID controller for an AVR using particle swarm optimization. Control Eng Pract. 2009;17:1380–7.
[24] Monje CA, Vinagre BM, Calderon AJ, Feliu V, Chen YQ. On fractional PI^{λ} controllers: some tuning rules for robustness to plant uncertainties. Nonlinear Dyn 2004;38:369–81.
[25] Barbosa RS, Tenreiro Machado JA, Ferreira IM. Tuning of PID controllers based on Bode's ideal transfer function. Nonlinear Dyn. 2004;38:305–21.
[26] Sekhar GTC, Sahu RK, Baliarsingh AK, Panda S. Load frequency control of power system under deregulated environment using optimal firefly algorithm. Int J Electr Power Energy Syst 2016;74:195–211.
[27] Ali ES, Abd-Elazim SM. Bacteria foraging optimization algorithm based load frequency controller for interconnected power system. Int J Electr Power Energy Syst 2011;33(3):633–8.
[28] Zadeh LA. The concept of a linguistic variable and its application to approximate reasoning-I. Inf Sci 1975;8(3):199–249.
[29] Bingul Z, Karahan O. A fuzzy logic controller tuned with PSO for 2 DOF robot trajectory control. Expert Syst Appl 2011;38(1):1017–31.
[30] Juang CF, Chang PH. Designing fuzzy-rule-based systems using continuous ant-colony optimization. IEEE Trans Fuzzy Syst 2010;18(1):138–49.
[31] Alomoush MI. Load frequency control and automatic generation control using fractional-order controllers. Electr Eng 2010;91:357–68.
[32] Vinagre BM, Podlubny I, Hernandez A, Feliu V. Some approximations of fractional order operators used in control theory and applications. Fract Calc Appl Anal 2000;3(3):231–48.